0026-895X/02/6201-48–57$7.00
MOLECULAR PHARMACOLOGY
Copyright © 2002 The American Society for Pharmacology and Experimental Therapeutics
Mol Pharmacol 62:48–57, 2002

Vol. 62, No. 1
1508/992248
Printed in U.S.A.

MOL PHARM

Novel Tarantula Toxins for Subtypes of Voltage-Dependent Potassium Channels in the Kv2 and Kv4 Subfamilies

PIERRE ESCOUBAS, SYLVIE DIOCHOT, MARIE-LOUISE CÉLÉRIER, TERUMI NAKAJIMA, and MICHEL LAZDUNSKI

Institut de Pharmacologie Moléculaire et Cellulaire, Centre National de la Recherche Scientifique-Unité Mixte Recherche 6097, Sophia-Antipolis, Valbonne, France (P.E., S.D., M.L.); Université Pierre et Marie Curie, Paris, France (P.E., M.-L.C.); and Suntory Institute for Bioorganic Research, Osaka, Japan (T.N.)

Received November 21, 2001; accepted April 4, 2002

This article is available online at http://molpharm.aspetjournals.org

ABSTRACT

Three novel peptides with the ability to inhibit voltage-dependent potassium channels in the *shab* (Kv2) and *shal* (Kv4) subfamilies were identified from the venom of the African tarantulas *Stromatopelma calceata* (ScTx1) and *Heteroscodra maculata* (HmTx1, HmTx2). The three toxins are 34- to 38-amino acid peptides that belong to the structural family of inhibitor cystine knot spider peptides reticulated by three disulfide bridges. Electrophysiological recordings in COS cells show that these toxins act as gating modifier of voltage-dependent K^+ channels. ScTx1 is the first high-affinity inhibitor of the Kv2.2 channel subtype (IC_{50}, 21.4 nM) to be described. ScTx1 also inhibits the Kv2.1 channels, with an IC_{50} of 12.7 nM, and Kv2.1/Kv9.3 heteromultimers that have been proposed to be involved in O_2 sensing in pulmonary artery myocytes. In addition, it is the most effective inhibitor of Kv4.2 channels described thus far, with an IC_{50} of 1.2 nM. HmTx toxins share sequence similarities with both the potassium channel blocker toxins (HmTx1) and the calcium channel blocker toxin ω-GsTx SIA (HmTx2). They inhibit potassium current associated with Kv2 subtypes in the 100 to 300 nM concentration range. HmTx2 seems to be a specific inhibitor of Kv2 channels, whereas HmTx1 also inhibits Kv4 channels, including Kv4.1, with the same potency. HmTx1 is the first described peptide effector of the Kv4.1 subtype. Those novel toxins are new tools for the investigation of the physiological role of the different potassium channel subunits in cellular physiology.

MOLECULAR PHARMACOLOGY

Downloaded from molpharm.aspetjournals.org by guest on December 1, 2012

In most cells, two types of depolarization-activated outward K^+ currents (Kv) are distinguished. Transient K^+ currents (I_A currents), which activate and inactivate rapidly, and delayed K^+ currents (I_K currents), which inactivate slowly. They contribute to several important functions in cardiac and neuronal physiology. In cardiac cells, this role more specifically concerns the height and duration of the plateau phase of the action potential, repolarization of cell membranes, cardiac refractoriness, and automaticity (Barry et al., 1998; Xu et al., 1999b). In the nervous system, I_A and I_K currents control the membrane resting potential, the firing pattern, and action potential duration and repolarization (Jan and Jan, 1989). Thus, they are implicated in membrane excitability, hormone release, and signal transduction and processing.

To date, more than 70 mammalian genes encoding K^+ channels have been cloned. Four different subfamilies of genes (Kv1, Kv2, Kv3, and Kv4) encode functional voltage-dependent K^+ channels (Kv) (Jan and Jan, 1997). The Kv2 subfamily, consisting of Kv2.1 and Kv2.2 subtypes, encodes I_K currents (Frech et al., 1989; Pak et al., 1991b; Hwang et al., 1992), whereas the Kv4 subfamily, which comprises Kv4.1, Kv4.2, and Kv4.3, encodes only I_A currents (Baldwin et al., 1991; Pak et al., 1991a; Fiset et al., 1997; Serodio and Rudy, 1998). Functional Kv channels are tetramers of α subunits forming homo- or heteromultimeric channels. In the Kv2 subfamily, Kv2.1 can coassemble with Kv2.2 or with silent α1 subunits, such as Kv8.1, Kv9.1, Kv9.2, and Kv9.3, forming heteromultimeric channels with new biophysical properties, and may be implicated in physiological functions different from those of homomultimeric channels (Patel et al., 1997; Salinas et al., 1997; Blaine and Ribera, 1998; Hulme et al., 1999). Recent work has shown that association of Kv2.1 and Kv9.3 subunits in smooth muscle cells could produce oxygen-sensitive K^+ channels (Patel et al., 1997; Hulme et al., 1999; Patel et al., 1999) that play a critical role in hypoxia-induced vasoconstriction of resistance pulmonary artery smooth muscle.

The physiological role of some of the Kv channels is now better understood thanks to the discovery of animal toxins that bind with high affinity and specificity to the different Kv α1 subunits. The Kv1 subfamily has a rich toxin pharmacology (Moczydlowski et al., 1988; Pongs, 1992; Grissmer et al.,

This work was supported by the Centre National de la Recherche Scientifique (CNRS), the French Ministry of Research and Technology (MRT), and the Association Française contre les Myopathies (AFM).

ABBREVIATIONS: Kv, voltage-dependent potassium channels; I_A currents, transient K^+ currents; I_K currents, delayed K^+ currents; ScTx, stromatoxin; HmTx, heteroscodratoxin; TFA, trifluoroacetic acid; HPLC, high-performance liquid chromatography; TEA, tetraethyl ammonium.

MOL PHARM

MOLECULAR PHARMACOLOGY

1994) obtained from snake (Rehm and Lazdunski, 1988; Awan and Dolly, 1991), scorpion (Aiyar et al., 1995; Hidalgo and MacKinnon, 1995; Miller, 1995; Tytgat et al., 1999), bee (Rehm et al., 1988), and sea anemone (Aneiros et al., 1993; Pennington et al., 1995; Schweitz et al., 1995; Alessandri-Haber et al., 1999) venoms. In the Kv2, Kv3, and Kv4 subfamilies, a number of "orphan" channels, such as Kv2.2, Kv3.1, Kv3.2, Kv3.3, or Kv4.1, still do not have specific ligands.

Kv2.1 is widely expressed in mammalian neurons and is present in the soma and proximal dendrites, particularly in hippocampus neurons (Murakoshi and Trimmer, 1999). Indirect evidence suggests a major role for Kv2.1 in the regulation of electrical transmission to and from the soma (Murakoshi and Trimmer, 1999). However, the specific contribution of Kv2.1 to delayed rectifier currents in neurons has not been investigated because of a lack of suitable pharmacological effectors. Although Kv2.1 and Kv2.2 colocalize in neurons (Hwang et al., 1993), they may have different cellular localizations and different roles in mediating delayed rectifier currents. Further investigation of the central role of these channels requires the development of a specific pharmacology.

Spider venoms are a unique source of toxins for Kv2.1, Kv4.2, and Kv4.3 channels (Swartz and MacKinnon, 1995; Sanguinetti et al., 1997; Diochot et al., 1999). Hanatoxins, heteropodatoxins, and phrixotoxins are short peptides, highly reticulated by disulfide bridges, that belong to the same structural family (Bernard et al., 2000; Escoubas et al., 2000; Takahashi et al., 2000) and share a similar mode of action. They modify the kinetics of either inactivation or activation gating through interaction with the voltage-sensing domain of Kv channels (Li-Smerin and Swartz, 1998; Winterfield and Swartz, 2000). The phrixotoxins were recently used to elucidate the exact role of I_A-type Ito current in cardiac function (Diochot et al., 1999).

This article describes the identification and properties of several novel tarantula toxins that are potent inhibitors of Kv2 and Kv4 channel subtypes. One of them, ScTx1, is a high affinity inhibitor for both I_A and I_K currents. ScTx1 is the first inhibitor described to date for the Kv2.2 channel. It also inhibits Kv2.1 channels and Kv2.1/9.3 heteromultimers with high affinity. Moreover, ScTx1 is a high-affinity inhibitor of transient Kv4.2 currents.

Materials and Methods

Biologicals. *Stromatopelma calceata* (formerly *Scodra griseipes*) (Sc) venom was obtained from homogenous groups of laboratory-bred adult female specimens using either electrical stimulation of chelicera or a lure-biting technique as described previously (Célérier et al., 1993). *Heteroscodra maculata* (Hm) venom was purchased from a commercial supplier (Invertebrate Biologics, Los Gatos, CA) and obtained by electrical stimulation of chelicera. Venom released from the fangs was collected in Eppendorf tubes and freeze-dried. All samples (dry weight ~25% of volume) were redissolved in distilled water to 1:10 the initial venom volume, centrifuged (14,000 rpm, 20 min), and filtered on 0.45 μm microfilters (Millipore Corporation, Bedford, MA). Venoms were subsequently stored at −20°C before analysis.

Toxin Purification and Characterization. For each venom, a 100-μl aliquot of the venom solution (10 μl of crude venom-equivalent) was fractionated by C8 reversed-phase semipreparative HPLC (5C8MS, 10 × 250 mm; Nacalai Tesque, Kyoto, Japan) using a linear gradient of water (A)/acetonitrile (B) in constant 0.1% TFA (0–60% B in 60 min) and fractions were hand-collected by monitoring the effluent signal. Aliquots of each fraction were assayed for activity against Kv2 channels expressed in the *Xenopus laevis* oocyte system and active fractions were further separated by cation-exchange chromatography on a Tosoh SP5PW column (4.6 × 70 mm; Tosoh, Tokyo, Japan), with a linear gradient of ammonium acetate in water (20 mM to 1 M in 50 min). A third purification step was conducted for toxin ScTx1 using a reversed-phase column (symmetry C18; Waters, Milford, MA) and a linear gradient of acetonitrile in water and 0.1% TFA (0–15% B in 15min, 15–40% B in 50 min). All solvents used were of HPLC grade. Separations were conducted on a HP1100 system (Hewlett Packard, Palo Alto, CA) coupled to a diode-array detector and a microcomputer running the Chemstation software (Agilent Technologies, Palo Alto, CA). Monitoring of the elution was done at 215 and 280 nm. Additional amounts of toxins were purified from a second batch of 100 μl of crude *S. calceata* venom and 20 μl of crude *H. maculata* venom using the same protocol.

For sequencing, the peptides were reduced and alkylated by 4-vinylpyridine, desalted by C8 reversed phase-HPLC, and submitted to automated N-terminal sequencing on a gas-phase sequencer (model 477A; Applied Biosystems, Foster City, CA).

Sequence homologies were determined using sequences obtained from literature data and a search of nonredundant protein databases, via the BLAST server (http://www.ncbi.nlm.nih.gov/BLAST/). Sequence alignments and percentages of similarity were calculated with ClustalW (http://www2.ebi.ac.uk/clustalw/) and a phylogenetic tree was constructed using the TreeView program.

Matrix-Assisted Laser Desorption-Ionization Time-of-Flight Mass Spectrometry. Peptides mixed with α-cyano-4-hydroxycinnamic acid (Sigma-Aldrich, St. Louis, MO) matrix [1:5 (v/v)] were analyzed on an Applied Biosystems Voyager DE-Pro system in reflector mode. Mass spectra (200–300 scans) were calibrated with internal standards and analyzed in the Data Explorer software.

Homology Modeling. Three-dimensional models of ScTx1 and HmTx1 were calculated using the NMR structure coordinates of hanatoxin 1 (PDB code 1D1H) as a template. Initial backbone fitting and energy minimization steps were performed with the DeepView program (Swiss-PDB Viewer; http://www.expasy.ch/spdbv/) and further refined via submission to the Swiss-Model server (http://www.expasy.ch/swissmod/SWISS-MODEL.html). Estimation of model reliability, calculation of electrostatic potentials and model exploration were carried using the DeepView and RasMol (http://www.openrasmol.org/) programs.

Oocyte Injection and Cell Transfections. cRNA synthesis and oocyte preparation were done as described previously (Salinas et al., 1997). For screening purposes, *X. laevis* oocytes were injected with 2.5 ng of Kv2.1 or 10 ng of Kv2.2 cRNA. Two days before transfection, COS M6 cells were plated at a density of 20,000/culture dish on cover glasses and transfected by a modification of the DEAE-dextran/chloroquine method as described previously (Fink et al., 1996; Patel et al., 1997; Diochot et al., 1999). We used the following plasmid DNA: pCI-Kv2.n (0.01 μg), pCI-Kv9.3-CD8 (0.03 μg), pCI-Kv4.n (0.05 μg), pCI-Kv1.1 (0.01 μg), pCI-Kv1.2 (0.05 μg), pCI-KV1.3 (0.005 μg), pCI-Kv1.4 (0.01 μg), pCI-Kv1.5 (0.05 μg), pCI-Kv1.6 (0.01 μg), pCI-KvLQT1 (0.1 μg), pRc-CMV-Kv3.4 (0.005 μg). A CD8-expressing plasmid (0.01 to 0.1 mg) was added in all transfection experiments, except for pCI-Kv9.3-CD8, to visualize transfected cells using anti-CD8 antibody-coated beads. Currents were recorded within 1 to 2 days after transfection.

Preparation of Rat Granular Cells. Cerebellar granule cells were grown in primary culture after enzymatic and mechanical dissociation from 6 -ay-old Wistar rats. Dissected cerebella were incubated in a 0.1% trypsin (Sigma) and 0.1% DNase (Sigma) in Ca^{2+}- and Mg^{2+}-free Krebs' solution for 10 min at 37°C. Cerebella were dissociated mechanically by trituration through a fire-polished Pasteur pipette to obtain single cell suspensions, which were centri-

Downloaded from molpharm.aspetjournals.org by guest on December 1, 2012

MOL PHARM

MOLECULAR PHARMACOLOGY

fuged at 1000 rpm for 5 min and resuspended in fresh media. The cells were plated on precoated glass coverslips with 25 μg/ml poly(L-lysine) (Sigma) and kept in minimal essential medium supplemented with 10% fetal calf serum, 25 mM KCl, 2 mM glutamine, 6 g/l glucose, 62.5 mg/l penicillin, and 50 mg/l streptomycin. Cytosine arabinoside (10 μM) was added to the culture 48 h after plating to inhibit the proliferation of non-neuronal cells. Experiments were performed on granular cells grown from 15 to 20 days in vitro.

Electrophysiological Measurements. For oocyte recordings, currents were measured by the two-microelectrode voltage-clamp technique. Venoms were diluted (1/1000) in ND96 saline solution. Electrophysiological measurements on COS transfected cells were performed 48 h after transfection using the whole-cell configuration of the patch-clamp technique. The pipette solution used was 150 mM KCl, 3 mM $MgCl_2$, 5 mM EGTA, and 10 mM HEPES-KOH, at pH 7.4. The extracellular solution composition was: 5 mM KCl, 150 mM NaCl, 1 mM $CaCl_2$, 3 mM $MgCl_2$, and 10 mM HEPES-NaOH, pH 7.4. Bovine serum albumin (0.1%) was added in toxin-containing solutions to prevent adsorption. The Kv current-voltage curves were determined by applying 10-mV incremental depolarizing pulses from a holding potential of −80 mV. Kv2.n current amplitudes were measured at 500-ms depolarization pulses. Kv4.n peak transient currents elicited by depolarizations, were measured after digital leak subtraction calculated at the end of depolarization (at 300 ms). All averaged data are presented as mean ± S.E.M.

For calcium currents recordings, the bath solution contained 10 mM $BaCl_2$, 135 mM TEACl, and 10 mM HEPES-TEAOH, pH 7.4. For sodium currents recordings, the external solution contained (in mM): NaCl 50, $MgCl_2$ 1, $CaCl_2$ 1.8, TEACl 100, HEPES-TEAOH 10, pH 7.4. For both calcium and sodium currents the pipette solution contained 100 mM CsCl, 5 mM $MgCl_2$, 10 mM EGTA, 4 mM ATP, and 30 mM HEPES-CsOH, pH 7.4.

Na^+ and Ca^+ currents were measured by applying depolarizing pulses from a holding potential of −90 mV in the whole cell configuration of the patch clamp technique. Na^+ currents were elicited by depolarizations between −60 and 0 mV, Ca^+ currents by depolarization between −30 and + 20 mV.

Mouse Intracerebroventricular Assay. Five-week-old Balb/C mice (average weight, ~20 g) were injected in the left cerebral ventricle with a 10-μl precision syringe fitted with a glass stopper. Samples (5 μl) were dissolved in a solution of bovine serum albumin (20 g/l in 9% NaCl) and were injected at a dose of 100 and 500 pmol/mouse. Mice were anesthetized with diethyl ether before injection and were placed in glass jars for observation. Symptoms were noted continuously during the first hour after injection and were monitored at regular intervals for 24 h or until death.

Results

Isolation and Structural Characterization of Hm and Sc Toxins. As part of a search for new pharmacological tools for K^+ channels, a large-scale screening of tarantula venoms on Kv2 channels expressed in *X. laevis* oocytes was undertaken. It singled out venoms from the African arboreal tarantulas *H. maculata* and *S. calceata* as particularly potent and durable inhibitors of Kv2.1 currents.

Bioassay-guided fractionation of crude venom after Kv2.1 inhibition located the activity in fraction 20 of *S. calceata* (~30% acetonitrile) (Fig. 1A) and fractions 22 and 23 of *H. maculata* (~35% acetonitrile) (Fig. 1B). These fractions yielded three toxins that were essentially pure after the second chromatography step (Fig. 1C). Their full sequence was obtained in a single run of Edman sequencing and confirmed by mass spectrometry (Fig. 2A). Toxin ScTx1 [Stromatoxin 1 (*S. calceata*)] is a 34 amino acid peptide reticulated by three disulfide bridges. Its measured monoisotopic molecular mass (3788.62 Da) is in accordance with the value calculated for an amidated C terminus (3788.56 Da). Toxins HmTx1 and HmTx2 [Heteroscodratoxins 1 and 2 (*H. maculata*)] are composed, respectively, of 35 and 38 amino acids, cross-linked by three disulfide bridges. Calculated monoisotopic molecular masses (3994.57 and 4754.06 Da) are in accordance with measured values (3994.59 and 4754.09 Da), indicating a carboxylated C terminus for HmTx1 and an amidated C terminus for HmTx2. Although the pairing of cysteines was not determined experimentally, the high homology of structure with previously described tarantula toxins strongly suggests that the peptides conform to the canonical inhibitor cystine knot Cys1-Cys4/Cys2-Cys5/Cys3-Cys6 disulfide bridge pattern (Norton and Pallaghy, 1998; Escoubas et al., 2000).

ScTx1 and HmTx1 are both basic peptides (pI, 9.70 and 7.69, respectively) while HmTx2 is an acidic peptide (pI, 4.95). Alignment with other Kv2 and Kv4 toxins shows that ScTx1 has the highest homology with hanatoxin 1 (83.2% similarity); that HmTx1 shares significant homology with SgTx1 (93.4%), a K^+ channel blocker previously isolated from the same venom (Marvin et al., 1999); and that HmTx2 resembles ω-grammotoxin SIA (76.1%), a calcium channel blocker from the venom of the Chilean tarantula *Grammostola spatulata* (Lampe et al., 1993). Homology modeling was successful for ScTx1 and HmTx2 but could not be completed for HmTx2 because of the lack of a suitable template.

Effects of ScTx1 and HmTx on Kv2.2 Channels. The pharmacological effects of ScTx1, HmTx2, and HmTx1 peptides were characterized on Kv2.2 currents recorded in COS cells by the whole-cell patch-clamp technique. The Kv2.2 current is partially inhibited by HmTx1 at 100 nM (19 ± 7%, n = 4 at 0 mV) and half-inhibited by a concentration of 300 nM (51 ± 9%, n = 4); the Kv2.2 current is not reduced by HmTx2 at concentrations up to 300 nM. ScTx1 is the most potent of the three toxins and totally inhibits the Kv2.2 current at a concentration of 100 nM (Fig. 3B).

Conductance-voltage curves show that the Kv2.2 currents activate around −30 mV with a maximum amplitude at + 40 mV and a $V_{0.5}$ = −3 ± 4 mV (Fig. 3A). The dose-response curve of Kv2.2 current inhibition by ScTx1 at 0 mV yielded an IC_{50} value of 21.4 nM [Hill coefficient (n_H) = 1.04] (Fig. 3, B and C). This inhibition is rapid (steady-state inhibition occurred after 113 ± 30 s at a concentration of 30 to 100 nM, n = 7) and slowly reversible. The effects of ScTx1 on Kv2.2 channels are voltage-dependent because the inhibition is maximal between −30 and 0 mV and incomplete at voltages over + 10 mV. This effect is illustrated by the shift of the conductance-voltage curve toward positive potentials (Fig. 3D).

ScTx1 Also Inhibits Kv2.1 Channels. The complete effects of ScTx1, HmTx2, and HmTx1 were also investigated on Kv2.1 currents recorded in COS cells. Conductance-voltage curves show that the Kv2.1 currents activate around −30 mV with a maximum amplitude at + 40 mV and a $V_{0.5}$ = 0.6 ± 4 mV (n = 20) (Fig. 4A). The pharmacological properties of the toxins are nearly the same as for Kv2.2 currents and they inhibit the Kv2.1 current with the same order of potency (ScTx1 > HmTx1 > HmTx2). HmTx1 inhibits 23 ± 5% (n = 5) of the current at a concentration of 100 nM, whereas HmTx2 at a concentration of 300 nM has a weak activity on the Kv2.1 current evoked at 0 mV (inhibition 18 ± 4%; n = 4).

Downloaded from molpharm.aspetjournals.org by guest on December 1, 2012

ScTx1 is a very potent inhibitor of the Kv2.1 current as shown by its dose-response curve with an IC_{50} value of 12.7 nM determined at $V_{0.5}$ (0 mV; n_H = 1.26) (Fig. 4, B and C). These effects are rapid (steady state reached in 101 ± 20 s at a concentration of 10 to 100 nM, n = 15) and almost totally but slowly reversible upon washout (Fig. 4D). ScTx1 inhibits the Kv2.1 current in a voltage-dependent manner, similarly to Kv2.2. This inhibition results from a shift of the activation curve to more positive potentials and therefore a fraction of the Kv2.1 current (~20–30%) remains unblocked at high depolarizing voltages (> +40 mV) (Fig. 4, E and F).

Effect of ScTx1 on the Kv2.1/9.3 Heteromultimer. Kv9.3 is a Kv2-like subunit that can associate with Kv2.1 and modulates its biophysical properties. As described previously (Patel et al., 1997, 1999), cells transfected with Kv9.3 alone do not express any channel activity, but when Kv9.3 is coexpressed with Kv2.1, potassium currents are measured and their activation threshold is shifted toward negative values (−50mV) (Fig. 5A). Currents are half-activated at $V_{0.5}$ = −18 ± 3 mV (n = 21), which represents a shift of 19 mV compared with homomultimeric Kv2.1 channels ($V_{0.5}$ = 0.6 ± 4 mV). Moreover, Kv2.1/9.3 channels generate currents with

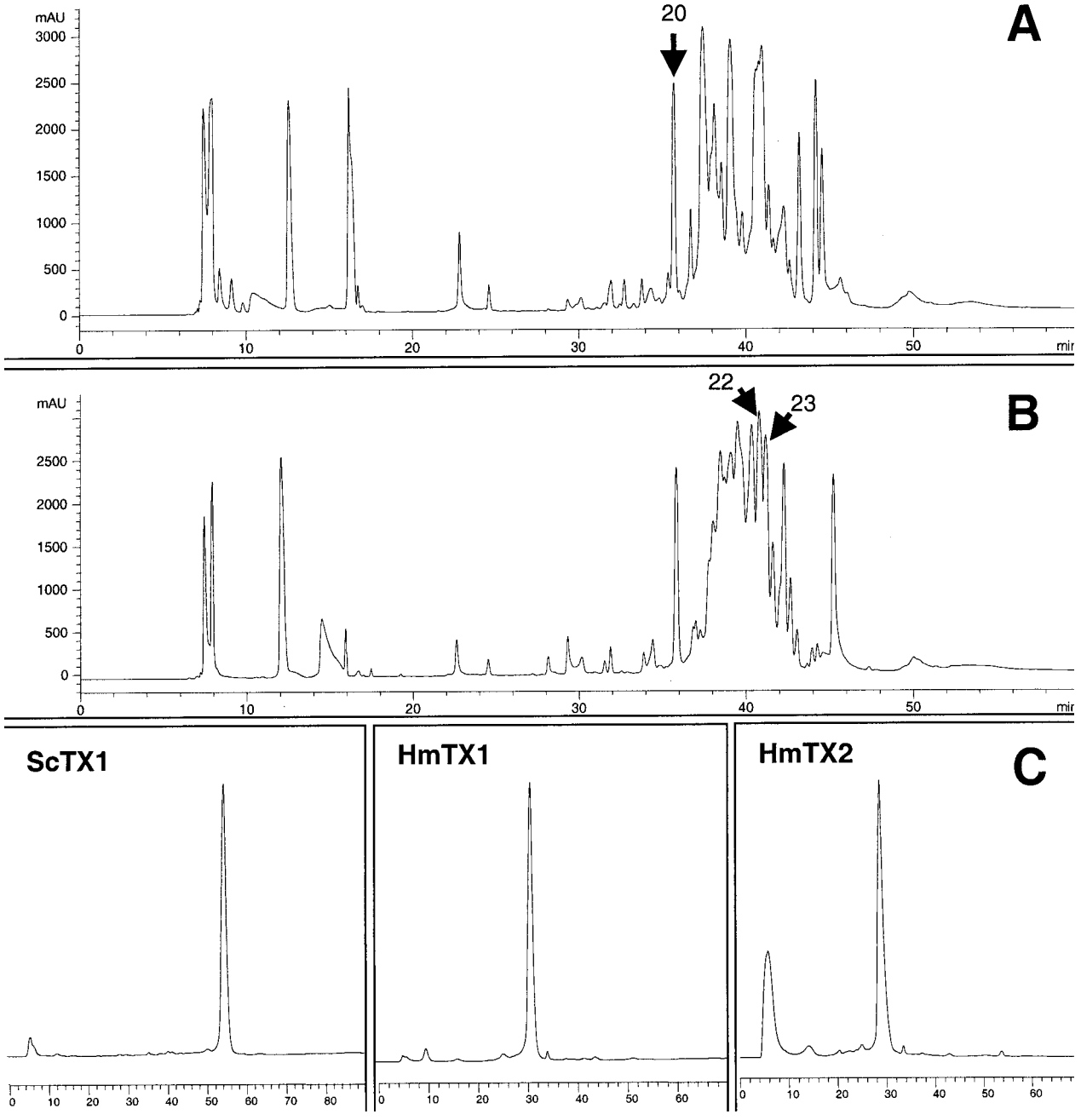

Fig. 1. Purification and characterization of ScTx1, HmTx1 and HmTx2. A, reversed-phase HPLC separation of crude *S. calceata* venom (10 μl) with a linear gradient of water/acetonitrile in 0.1% aqueous TFA. Arrow indicates the fraction (20) containing ScTx1 (215 nm). B, reversed-phase HPLC separation of crude *H. maculata* venom (10 μl) (similar conditions). Arrows indicate the fractions containing HmTx1 (22) and HmTx2 (23). C, cation-exchange chromatography of active fractions from A and B with a linear gradient of ammonium acetate (20 mM to 1M in 50 min, 280 nm).

MOL PHARM
MOLECULAR PHARMACOLOGY
aspet
Downloaded from molpharm.aspetjournals.org by guest on December 1, 2012

MOL PHARM
MOLECULAR PHARMACOLOGY
aspet

enhanced amplitude. Their activation kinetics are accelerated and their deactivation kinetics are slowed. We found that ScTx1 is also a potent inhibitor for the Kv2.1/9.3 heteromultimer. The dose-response curve was determined at −20 mV which corresponds to $V_{0.5}$ for Kv2.1/9.3. ScTx1 has a higher affinity for the heteromultimer, with an IC_{50} value of 7.2 nM (n_H = 1.08) (Fig. 5, B and C). As observed for the Kv2.1 homomultimer, the inhibition is rapid (steady state reached in 115 ± 19 s at a concentration of 10 to 100 nM, n = 12) and slowly reversible (Fig. 5D). ScTx1 at 100 nM can totally inhibit the Kv2.1/9.3 current evoked between −40 and 0 mV and only partially at depolarizing potentials over 0 mV (Fig. 5, E and F).

Effects of ScTx1, HmTx1, and HmTx2 on the Kv4 Subfamily. The hanatoxins act on both Kv2.1 and Kv4.2 channels (Swartz and MacKinnon, 1995) and the phrixotoxins, which share structural features with ScTx1, HmTx1, and HmTx2, inhibit Kv4.2 and Kv4.3 channels (Diochot et al., 1999) (Table 1). We tested the activity of ScTx1, HmTx1, and HmTx2 on Kv4.1, Kv4.2, and Kv4.3 currents recorded in transfected COS cells. All these currents activate and inactivate rapidly. Their activation threshold is around −40 mV and their $V_{0.5}$ is between −10 mV and 0 mV. Toxin activity was tested on Kv4 currents evoked at 0 mV. Among the three toxins tested at 100 nM, only HmTx1 is able to inhibit the Kv4.1 channel but with a relatively low affinity (IC_{50} = 280 nM, n_H = 0.73) as shown in Fig. 6, A and B; however, this is the first toxin reported to inhibit the Kv4.1 channel subtype to date.

The Kv4.3 currents were insensitive to HmTx2 and ScTx1 (100 nM, n = 5 each) but they were partially inhibited by HmTx1 at high concentrations (43 ± 8% at 300 nM, n = 3, data not shown). Kv4.2 currents were weakly sensitive or insensitive to high concentrations (100–300 nM) of HmTx1 (39 ± 3%, n = 4) and HmTx2 (no inhibition). Conversely, ScTx1 is a very potent inhibiter of Kv4.2. The dose-response curve for the inhibition of Kv4.2 by ScTx1 yielded an IC_{50} value of 1.2 nM (n_H = 0.98) (Fig. 6, C and D) (Table 1). The current is rapidly inhibited (steady state reached in 93 ± 20 s at a concentration of 3 to 30 nM, n = 7) and the effect is reversible upon washout. The mode of action of ScTx1 on Kv4.2 channels is comparable with that observed on Kv2.1 channels. The toxin induced a shift in the conductance-voltage relationship to more depolarized potentials (Fig. 6, E and F).

Absence of Inhibition of Other K^+ Channels. In order to determine their specificity, the toxins were tested on members of the Kv1 and Kv3 subfamilies of K^+ channels. In COS

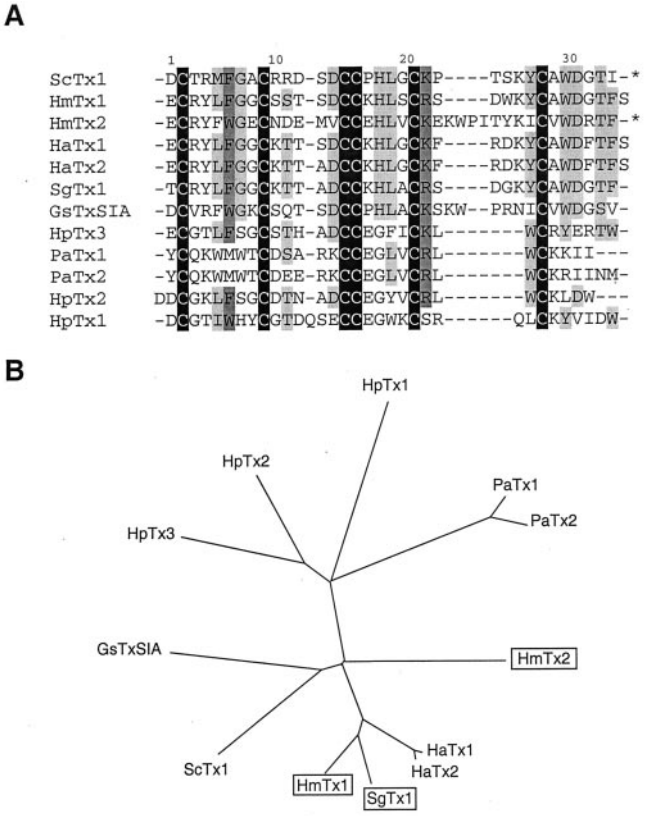

Fig. 2. Sequence alignment of ScTx1, HmTx1, and HmTx2. A, multiple alignment with short spider peptides of similar structure and known mode of action. Black boxes indicate conserved residues and gray boxes functionally homologous residues (*, C-terminal amidation). Sequences from Sanguinetti et al., 1997 (HpTx1, 2, 3; *Heteropoda venatoria*), Diochot et al., 1999 (phrixotoxins 1, 2; *Phrixotrichus auratus*), Swartz and MacKinnon, 1995 (hanatoxins 1, 2; *Grammostola spatulata*), Lampe et al., 1993 (GsTxSIA), Marvin et al., 1999 (SgTx1; *Scodra griseipes* = *S. calceata*). All peptides except HpTx1, 2, and 3 are from tarantula venoms. B, unrooted phylogenetic tree of tarantula toxins based on a ClustalW multiple alignment (see *Materials and Methods*).

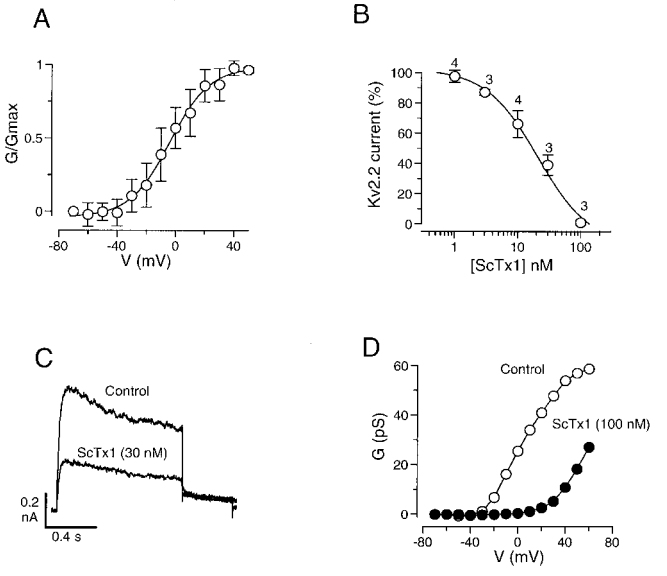

Fig. 3. Effect of ScTx1 on Kv2.2 currents. Kv2.2 currents were recorded in transfected COS cells in the whole-cell patch-clamp configuration. Holding potential, −80 mV. A, normalized and average conductance-voltage relationship for Kv2.2 current in control conditions. Conductances were measured on the tail current upon repolarization to −40 mV. The curve was fitted with the equation $G = G_{max} / [1 + \exp(V_{0.5} - V) / k]$, where $V_{0.5}$ is the midpoint potential and k is the curve slope. G was normalized to the peak membrane conductance at + 50 mV (G_{max}). For Kv2.2 current, $V_{0.5}$ is −3 ± 4 mV. B, Concentration-response relationship for ScTx1 inhibition of the Kv2.2 current evoked at 0 mV. The dose-response curve was fitted by the Hill equation: $I = I_{max} + (I_{min} - I_{max}) / [1 + (IC_{50} / C^{nH})]$, where I is the amplitude of the peak current, I_{max} and I_{min} are the amplitudes of the current corresponding to control and saturating concentrations of ScTx1, C is the concentration of the toxin, IC_{50} is the concentration of the toxin that corresponds to 50% I_{max}, and n_H is the Hill number (n_H = 1.04). Each point is the mean ± S.E.M. of data from three to four cells. C, effect of 30 nM ScTx1 on Kv2.2 current, recorded at a test pulse of 0 mV. D, conductance-voltage relationship for Kv2.2 current measured before (○) and during (●) application of 100 nM ScTx1.

Downloaded from molpharm.aspetjournals.org by guest on December 1, 2012

MOL PHARM
MOLECULAR PHARMACOLOGY
aspet

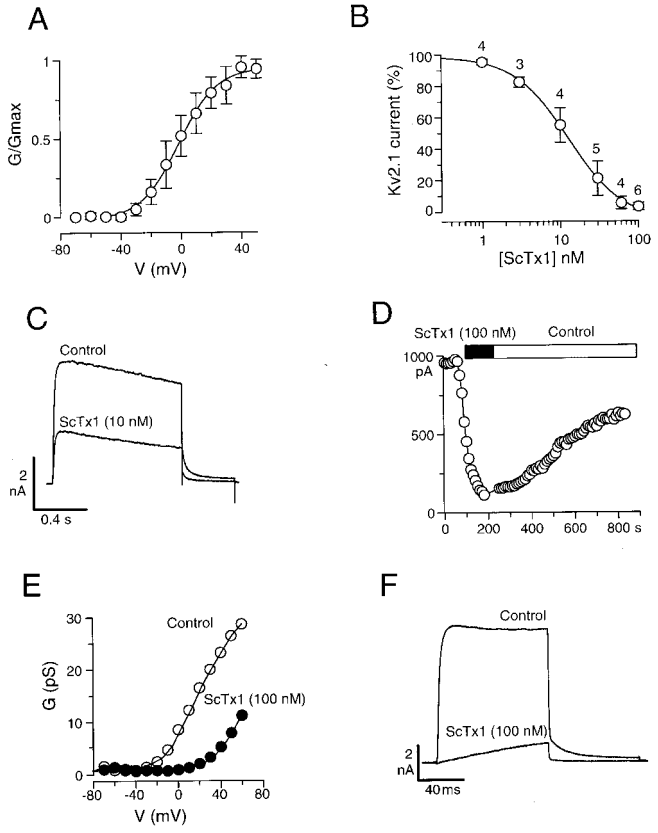

Fig. 4. Effect of ScTx1 on Kv2.1 currents. Effects were recorded in transfected COS cells in the whole-cell configuration. Holding potential, −80 mV. A, normalized and average conductance-voltage relationship for Kv2.1 current in control conditions. Conductances were measured on the tail current upon repolarization to −40 mV. The $V_{0.5}$ value determined from the equation in the legend to Fig. 3 is 0.6 ± 4 mV. B, concentration-response relationship for ScTx1 inhibition of the Kv2.1 current at 0 mV. Each point is the mean ± S.E.M. of data from three to six cells. The IC_{50} determined from the Hill equation (Fig. 3) is 12.7 nM (n_H = 1.26). C, effect of 10 nM ScTx1 on Kv2.2 current, recorded at a test pulse of 0 mV. D, time course for Kv2.1 current inhibition with 100 nM ScTx1 and reversibility. The amplitude of Kv2.1 was measured at 500 ms upon depolarization at 0 mV. E, conductance-voltage relationship for Kv2.1 current measured before (○) and during (●) application of 100 nM ScTx1. F, effect of 100 nM ScTx1 on Kv2.2 current, recorded at a test pulse of +50 mV.

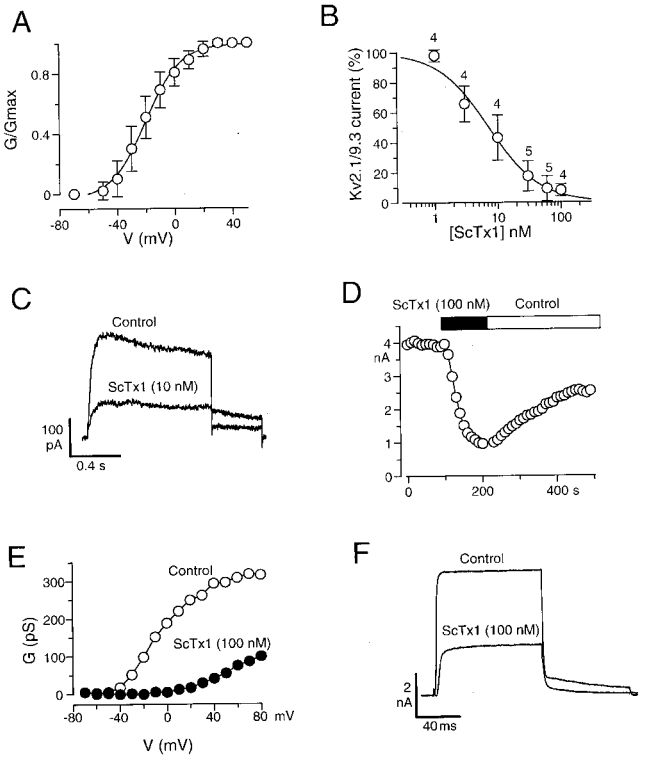

Fig. 5. Effect of ScTx1 on Kv2.1/9.3 heteromultimers. Currents were recorded in transfected COS cells in the whole-cell configuration. Holding potential, −80 mV. A, normalized and averaged conductance-voltage relationship for Kv2.1/9.3 current in control conditions. Conductances were measured on the tail current upon repolarization to −40 mV. The $V_{0.5}$ value determined from the equation in the legend to Fig. 3 is −18 ± 3 mV. B, concentration-response relationship for ScTx1 inhibition of the Kv2.1/9.3 current at −20 mV. Each point is the mean ± S.E.M. of data from four to five cells. The IC_{50} determined from the Hill equation (Fig. 3) is 7.2 nM (n_H = 1.08). C, effect of 10 nM ScTx1 on Kv2.1/9.3 current, recorded at a test pulse of −20 mV in outside-out configuration. D, time course for Kv2.1/9.3 current inhibition with 100 nM ScTx1 and reversibility. The amplitude of Kv2.1/9.3 was measured at 500 ms upon depolarization at +10 mV. E, conductance-voltage relationship for Kv2.1/9.3 current measured before (○) and during (○) application of 100 nM ScTx1. F, effect of 100 nM ScTx1 on Kv2.1/9.3 current, recorded at a test pulse of +50 mV.

TABLE 1

Activity of spider toxins on Kv2 and Kv4 channel subtypes

Activities of spider toxins against different subtypes of Kv2 and Kv4 potassium channels are reported as IC_{50} (nanomolar)or as percentage of current inhibition at a single dose (nanomolar). Affinity (IC_{50}) measurements obtained in electrophysiological experiments were obtained using a single site relation model (Hill relation, n_H = 1). Data are from this study (ScTx1, HmTx1, 2) or from previously published work for hanatoxin 1 (HaTx1; Swartz and MacKinnon, 1995), phrixotoxins (PaTx1, 2; Diochot et al., 1999), and heteropodatoxins (HpTx1, 2, 3; Sanguinetti et al., 1997).

Toxin	Kv2.1	Kv2.2	Kv2.1/9.3	Kv4.1	Kv4.2	Kv4.3
ScTx1	12.7	21.4	7.2	—	1.2	—
HmTx1	23% (100 nM)	19.7% (100 nM)	N.T.	280	39% (300 nM)	43% (300 nM)
HmTx2	18% (300 nM)	0% (300 nM)	N.T.	—	—	—
HaTx1	42	N.T.	N.T.	N.T.	70% (500 nM)[b]	N.T.
PaTx1	6% (500 nM)[a]	16% (500 nM)[a]	N.T.	39% (250 nM)	5	28
PaTx2	8% (500 nM)[a]	11% (500 nM)[a]	N.T.	20% (300 nM)	34	71
HpTx1	N.T.	N.T.	N.T.	N.T.	100	—
HpTx2	N.T.	N.T.	N.T.	N.T.	100	—
HpTx3	N.T.	N.T.	N.T.	N.T.	67	—

N.T., not tested; —, no activity.
[a] S. Diochot, unpublished observations.
[b] From Fig. 7, Swartz and MacKinnon (1995).

Downloaded from molpharm.aspetjournals.org by guest on December 1, 2012

MOL PHARM
MOLECULAR PHARMACOLOGY
aspet

cells transfected with Kv1.1, Kv1.2, Kv1.3, Kv1.4, Kv1.5, Kv1.6, and Kv1.2/Kv1.5 heteromultimers, KvLQT1 or Kv3.4 channels, we tested the toxins at concentrations of 100 and 300 nM. No significant effects (less than 20% inhibition) were observed either on the transient Kv1.3, Kv1.4, or Kv3.4 currents or on the sustained Kv1.1, Kv1.2, Kv1.5, Kv1.6, Kv1.2/Kv1.5, or KvLQT1 currents at 300 nM toxin concentration (n = 3 to 4 for each condition) (Table 2).

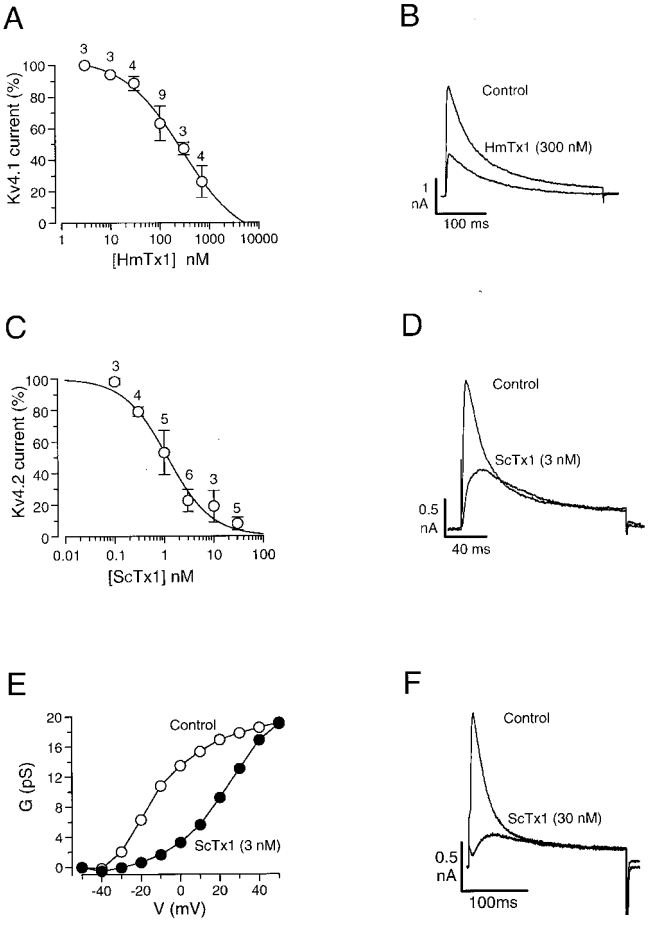

Fig. 6. Effect of HmTx1 on Kv4.1 current and inhibition of Kv4.2 currents by ScTx1. Kv4.1 and Kv4.2 currents were recorded in transfected COS cells in the whole-cell configuration. Holding potential, −80 mV. A, concentration-response relationship for HmTx1 inhibition of peak Kv4.1 current at 0 mV. Each point is the mean ± S.E.M. of data from three to nine cells. The IC_{50} determined from the Hill equation (Fig. 3) is 280 nM (n_H = 0.73). B, effect of 300 nM HmTx1 on Kv4.1 current, recorded at a test pulse of 0 mV. C, concentration-response relationship for ScTx1 inhibition of peak Kv4.2 current at 0 mV. Each point is the mean ± S.E.M. of data from three to six cells. The IC_{50} determined from the Hill equation (Fig. 3) is 1.2 nM (n_H = 0.98). D, effect of 3 nM ScTx1 on Kv4.2 current, recorded at a test pulse of 0 mV. E, conductance-voltage relationship for Kv4.2 current measured before (○) and during (●) application of 3 nM ScTx1. Conductances were calculated with the equation $G = I / (V - E_K)$ where G is the conductance, I the amplitude of peak Kv4.2 current, V is the test potential, and E_K is the reversal potential for K^+ (−85 mV). G was normalized to the peak membrane conductance at +50 mV (G_{max}). F, effect of 30 nM ScTx1 on Kv4.2 current, recorded at a test pulse of 0 mV.

In Vivo Effect of ScTx1. ICV injection of 100 or 500 pmol of ScTx1 or HmTx2 induced no observable neurotoxicity symptoms in mice monitored for 24 h. Conversely, injection of 500 pmol of HmTx1 induced the immediate appearance of convulsions, and death occurred in less than 1 h. Injection of a lower dose (100 pmol) also induced rapid convulsions (3 min), spasms, and tremors. Death occurred in less than 2 h after injection and was preceded by recurrent spasms and paralysis. Among the three toxins, HmTx1 was the only peptide to induce neurotoxic symptoms, indicating a significant difference in its mode of action.

Effects of ScTx1, HmTx1, and HmTx2 on Ca^{2+} and Na^+ Currents in Rat Cerebellar Granule Cells. High concentrations (100 nM) of the three toxins were tested on voltage-dependent Na^+ currents measured in cultured rat granular cells. Maximal rapidly activating and inactivating Na^+ currents were evoked by depolarization pulses of −40 mV and the toxins were perfused during 1 to 2 min. ScTx1, HmTx1, and HmTx2 were inactive against Na^+ currents (n = 4).

ScTx1, HmTx1, and HmTx2 were also tested at a concentration of 100 nM on voltage-dependent Ca^{2+} currents recorded in the same cells. Toxins were without effect (less than 5% inhibition, n = 5) on the maximal inward currents evoked by depolarizations at 0 mV.

Discussion

The Kv2.2 protein is found predominantly in the central nervous system (Hwang et al., 1993), but expression of the Kv2.2 gene has been detected in smooth muscle from rat mesenteric arteries (Xu et al., 1999a). The greatest density of Kv2.2 mRNA occurs in the olfactory bulb, the cerebral cortex, the hippocampus, and the cerebellum, but only in restricted areas of neurons (Hwang et al., 1992, 1993; Lim et al., 2000). ScTx1 is the first high-affinity peptide inhibitor of the Kv2.2 current with an IC_{50} of 21.4 nM to be described. In addition, ScTx1 is also the strongest inhibitor of Kv2.1 channels described thus far, with an IC_{50} of 12.7 nM (single site relation). Under the same set of calculation parameters, the hanatoxins were reported to inhibit Kv2.1 channels with an affinity of 42 nM (Swartz and MacKinnon, 1995), and subsequent reports using a four-site independent model have indicated half-inhibition values of 102 nM for the mixture of hanatoxins 1 and 2 and 160 nM for synthetic hanatoxin 1 (Swartz and MacKinnon, 1997a; Takahashi et al., 2000). Kv2.1 channels have been recognized recently as being the major contributors to the delayed-rectifier current in mammalian central neurons (Murakoshi and Trimmer, 1999). ScTx1 will proba-

TABLE 2
Effects of ScTx1, HmTx1, and HmTx2 on different potassium channels
Kv1.n , Kv3.4, and KvLQT1 channels were expressed in COS cells. Values are mean percentage current inhibition ± S.E.M. after application of toxins (300 nM; n = 3 to 5).

	Kv1.1	Kv1.2	Kv1.3	Kv1.4	Kv1.5	Kv1.6	Kv3.4	KvLQT1
					%			
ScTx1	8 ± 2	10 ± 4	9 ± 7	4 ± 3	0	0	4 ± 3	19 ± 5
HmTx1	12 ± 8	4 ± 1	3 ± 3	4 ± 3	2 ± 0.5	1 ± 1	4 ± 4	8 ± 4
HmTx2	10 ± 4	1 ± 1	6 ± 8	6 ± 4	1 ± 1	13 ± 9	2 ± 3	4 ± 2

Downloaded from molpharm.aspetjournals.org by guest on December 1, 2012

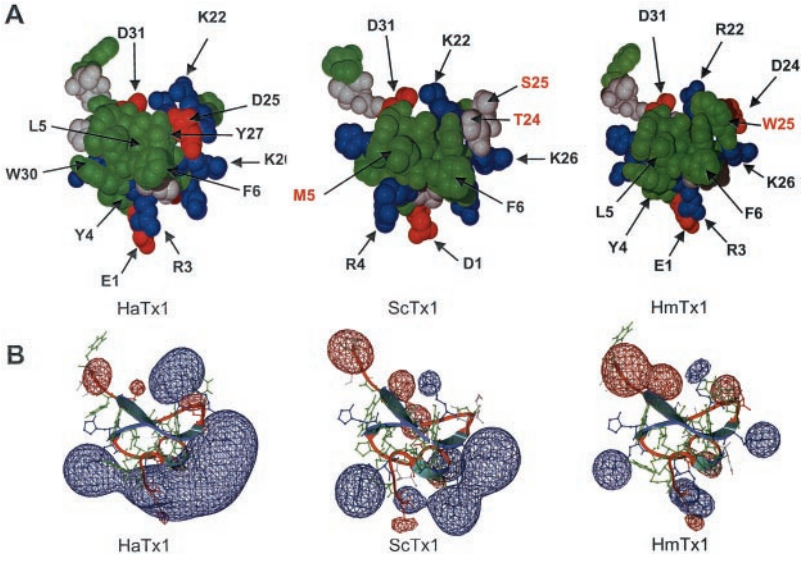

Fig. 7. A, Three-dimensional structure of hanatoxin 1, ScTx1, and HmTx1. Models of ScTx1 and HmTx1 were obtained by homology modeling based on the structure of hanatoxin 1 determined by NMR (PDB code 1D1H). CPK models were generated with RasMol. Residues are colored according to their properties. Blue, basic (Arg, Lys); Red, acidic (Glu, Asp); Green, hydrophobic (Ala, Cys, Ile, Leu, Met, Phe, Pro, Trp, Tyr, and Val). Residues are numbered according to ScTx1 sequence. B, electrostatic potential of hanatoxin 1, ScTx1, and HmTx1. Electrostatic potential maps of hanatoxin 1 (1D1H) and models of ScTx1 and HmTx1 are superimposed on ribbon diagrams of the toxin backbones. Blue, positive charges; red, negative charges. Electrostatic potential maps and structures were calculated with the DeepView program after homology modeling by the Swiss-Model server.

bly be an important tool for the identification of the functional role of Kv2 subunits in the brain as well as for further development of more selective agents that may be useful in the treatment of neurological disorders associated with Kv2 channel dysfunction.

We have also shown in this work that ScTx1 inhibits the heteromultimeric channel Kv2.1/9.3 with a high affinity (IC_{50} = 7.2 nM). This channel assembly has been shown to be present in pulmonary artery smooth muscle (Patel et al., 1999). Because ScTx1 has no activity on the Kv1.2/1.5 heteromultimer that has also been proposed as an O_2-sensing potassium channel (Hulme et al., 1999), its high affinity and selectivity toward Kv2.1/9.3 makes it an interesting tool to evaluate the relative contribution of different heteromultimeric channel assemblies in adaptive hypoxic mechanisms.

ScTx1 is also the most potent inhibitor known for the transient K^+ current Kv4.2 (IC_{50} = 1.2 nM). Phrixotoxins 1 and 2 inhibit Kv4.2 with IC_{50} values of 5 and 34 nM, respectively, and Kv4.3 with IC_{50} values of 28 and 71 nM. Heteropodatoxins have affinities in the 100 nM range (Sanguinetti et al., 1997) (Table 1). Interestingly, ScTx1 does not affect Kv4.3 channels, which, together with Kv4.2, have been demonstrated to underlie the Ito current in rodent cardiac myocytes (Diochot et al., 1999). Thus, ScTx1 used in combination with other, less specific Kv4 blockers, such as the phrixotoxins, will permit a better understanding of the respective contributions of Kv4.2 and Kv4.3 channels to the cardiac Ito current (Fiset et al., 1997; Diochot et al., 1999). ScTx1 could also be an excellent tool to allow a fine dissection of neuronal roles associated with Kv4.2 channels in brain.

ScTx1 acts by modulating the voltage-dependence of the channel and by inducing a shift in the conductance-voltage relationship to more depolarized potentials. ScTx1 slows both the activation and inactivation kinetics of the Kv4.2 current as illustrated by the crossover of the traces in Fig. 6D. Although their effects are quite different during strong depolarizations, ScTx1 somehow acts like 4-aminopyridine, which binds to the Kv4.2 channel in the closed state and unbinds in the activated state. The Hill coefficients obtained from the dose-response curves suggest that there is either one binding site for the toxins on the tetrameric channel or that there are four independent sites corresponding to each of the four subunits. The biophysical properties of channel inhibition by ScTx1 are very similar to those reported previously for hanatoxins, phrixotoxins or heteropodatoxins (Swartz and MacKinnon, 1995; Sanguinetti et al., 1997; Diochot et al., 1999). A common mode of action is emerging from the study of these different toxins. They all most probably interact with the voltage-sensing domain and with the S3–S4 extracellular loop in a manner similar to hanatoxins (Li-Smerin and Swartz, 1998). The ability of ScTx1 to potently inhibit both Kv2 and Kv4 channels with a similar mode of action suggests the presence of a conserved receptor surface on these channels.

Compared with ScTx1, toxins HmTx1 and HmTx2 from *H. maculata* venom showed a relatively lower activity against Kv2.1, although the whole venom strongly inhibited Kv2.1 expressed in oocytes because of the high abundance of these toxins in the venom. HmTx1 inhibits ~20–25% of Kv2.1 and Kv2.2 currents at 100 nM, whereas the IC_{50} of synthetic hanatoxin 1 on the same channel was reported to be 160 nM (Takahashi et al., 2000). HmTx2 is less active and does not affect Kv2.2 currents. The recent elucidation of the three-dimensional structure of hanatoxin 1 by NMR suggests that this toxin interacts with Kv2 channels via an hydrophobic surface comprising residues from loop I (Tyr4, Leu5, Phe6) associated with residues from the end of loop 4 (Tyr27) and the C-terminal end (Ala29, Trp30) to form the hydrophobic patch. This patch is surrounded by several positively and negatively charged residues that also interact with the channel receptor surface (Takahashi et al., 2000). Lys22 and Lys26 are completely conserved in ScTx1, HmTx1, and the hanatoxins, whereas Lys22 is replaced by an Arginine in HmTx1. Similarly, His18 is conserved in all toxins. Examination of the three-dimensional models (Fig. 7A) shows that another positive charge borne by Lys17 is present in this part of the molecule but can be replaced by a Proline in ScTx1. Another charged patch is formed by the dyad Glu1/Asp1 and a positive residue found in position 3 or 4. Although the geometry of the dyad changes, it is found in the three toxin types. Another highly conserved positive-negative dyad is formed by Asp31 and Lys22. A more variable charged region is observed in the vicinity of Asp25 in hanatoxins. Although the Asp residue is also found in HmTx1, it is replaced by

MOL PHARM
MOLECULAR PHARMACOLOGY
aspet
Downloaded from molpharm.aspetjournals.org by guest on December 1, 2012

MOL PHARM

MOLECULAR PHARMACOLOGY

Thr24 and Ser25 in ScTx1, a major change in the surface potential that most probably affects the selectivity of the toxin.

The hydrophobic residues that form the hydrophobic patch postulated to be involved in receptor recognition are highly conserved in all toxins (Tyr 4/Met5, Leu 5, Phe6, Ala29, and Trp30). The overall distribution of positive and negative surfaces (Fig. 7B) remains conserved for hanatoxin 1, ScTx1, and HmTx1, with a large positive surface near the N terminus of the molecule and a conserved spatial localization of the negative charges. Examination of the structures and surface properties of other toxins based on the inhibitor cystine knot fold and acting on Kv channels such as heteropodatoxin 2 (Bernard et al., 2000), shows a completely different surface potential distribution, although the two toxin types share a similar mode of action against Kv4 channels. Significant differences of size and sequence also separate these two families of toxins as shown in the tree presented in Fig. 2B. The combination of an hydrophobic surface surrounded by charged "anchors" can be proposed as a characteristic structural signature of this group of potassium channel inhibitors, and both basic and acidic residues (Asp1, Asp31 in ScTx1) seem to be involved in the formation of the charged ring surrounding the hydrophobic patch.

Although HmTx1 has only moderate activity on Kv4 channels, it is, interestingly, the first inhibitor of Kv4.1 channels described so far, with an IC_{50} of 280 nM. It is very likely that isoforms of this toxin with higher activity on Kv4.1 will be discovered in spider venoms.

HmTx1 is also the only one among the three toxins described in this work to demonstrate any toxicity in mice after ICV injection. This suggests that inhibition of Kv2.1, Kv2.2, and Kv4.2 channels does not lead to major neurotoxicity (ScTx1 and HmTx2) whereas inhibition of Kv4.1 would be more harmful, as with blockade of Kv1 channels by a variety of toxins (Bidard et al., 1987).

HmTx2 has a longer peptide chain and there is a notable increase in size of loop 4 (10 amino acids) compared with the toxins described above (6 amino acids). The additional loop also contains one negatively and two positively charged residues, and both the charge and the bulk of this loop will significantly affect the shape and charge distribution of the toxin. Because the pharmacological properties of HmTx2 differ from those of the other Kv2 toxins, it is conceivable that loop 4 may play an important role in channel discrimination. There is a possibility that HmTx2 may not be a potassium channel toxin but may possess a higher affinity for another as-yet-undetermined molecular target.

As previous studies have demonstrated, gating modifier toxins from spider venoms may interact with voltage-dependent potassium, calcium and sodium channels, probably via recognition of a conserved binding site on voltage-sensing domains. Hanatoxins and ω-grammotoxin SIA have been shown to interact with both voltage-gated K^+ and Ca^{2+} channels at high concentrations (Swartz and MacKinnon, 1997a,b; Li-Smerin and Swartz, 1998). Assessment of the activity of the three toxins against voltage-dependent calcium and sodium channels in rat cerebellar granule cells shows that neither toxin (at 100 nM) significantly affects the total calcium or sodium channel currents present in those cells.

Tarantula venoms are rich sources of Kv2 and Kv4 channel inhibitors. The study of additional venoms will undoubtedly lead to the discovery of an array of closely related toxins with slightly different pharmacological profiles providing tools for the elucidation of the respective physiological role of the different potassium channels subunits. These toxins will also help the analysis of the molecular mechanism of voltage-dependent channel gating.

Acknowledgments

We are grateful to M. Jodar, Y. Benhamou, and V. Lopez for technical assistance and to D. Moinier for assistance with peptide sequencing.

References

Aiyar J, Withka JM, Rizzi JP, Singleton DH, Andrews GC, Lin W, Boyd J, Hanson DC, Simon M, Dethlefs B, et al. (1995) Topology of the pore-region of a K^+ channel revealed by the NMR-derived structures of scorpion toxins. *Neuron* **15:**1169–1181.

Alessandri-Haber N, Lecoq A, Gasparini S, Grangier-Macmath G, Jacquet G, Harvey AL, de Medeiros C, Rowan EG, Gola M, Menez A, et al. (1999) Mapping the functional anatomy of BgK on Kv1.1, Kv1.2 and Kv1.3. Clues to design analogs with enhanced selectivity. *J Biol Chem* **274:**35653–35661.

Aneiros A, Garcia I, Martinez JR, Harvey AL, Anderson AJ, Marshall DL, Engstrom A, Hellman U, and Karlsson E (1993) A potassium channel toxin from the secretion of the sea anemone *Bunodosoma granulifera*. Isolation, amino acid sequence and biological activity. *Biochim Biophys Acta* **1157:**86–92.

Awan KA and Dolly JO (1991) K^+ channel sub-types in rat brain: characteristic locations revealed using beta-bungarotoxin, alpha- and delta-dendrotoxins. *Neuroscience* **40:**29–39.

Baldwin TJ, Tsaur ML, Lopez GA, Jan YN, and Jan LY (1991) Characterization of a mammalian cDNA for an inactivating voltage-sensitive K^+ channel. *Neuron* **7:**471–483.

Barry DM, Xu H, Schuessler RB, and Nerbonne JM (1998) Functional knockout of the transient outward current, long-QT syndrome and cardiac remodeling in mice expressing a dominant-negative Kv4 alpha subunit. *Circ Res* **83:**560–567.

Bernard C, Legros C, Ferrat G, Bischoff U, Marquardt A, Pongs O, and Darbon H (2000) Solution structure of HpTX2, a toxin from *Heteropoda venatoria* spider that blocks Kv4.2 potassium channel. *Protein Sci* **9:**2059–2067.

Bidard J-N, Mourre C, and Lazdunski M (1987) Two potent central convulsant peptides, a bee venom toxin, the MCD peptide and a snake venom toxin, dendrotoxin I, known to block K^+ channels, have interacting receptor sites. *Biochem Biophys Res Commun* **143:**383–389.

Blaine JT and Ribera AB (1998) Heteromultimeric potassium channels formed by members of the Kv2 subfamily. *J Neurosci* **18:**9585–9593.

Célérier ML, Paris C, and Lange C (1993) Venom of an aggressive African Theraphosidae (*Scodra griseipes*): milking the venom, a study of its toxicity and its characterization. *Toxicon* **31:**577–590.

Diochot S, Drici MD, Moinier D, Fink M, and Lazdunski M (1999) Effects of phrixotoxins on the Kv4 family of potassium channels and implications for the role of Ito1 in cardiac electrogenesis. *Br J Pharmacol* **126:**251–263.

Escoubas P, Diochot S, and Corzo G (2000) Structure and pharmacology of spider venom neurotoxins. *Biochimie* **82:**893–907.

Fink M, Duprat F, Lesage F, Reyes R, Romey G, Heurteaux C, and Lazdunski M (1996) Cloning, functional expression and brain localization of a novel unconventional outward rectifier K^+ channel. *EMBO (Eur Mol Biol Organ) J* **15:**6854–6862.

Fiset C, Clark RB, Shimoni Y, and Giles WR (1997) Shal-type channels contribute to the Ca^{2+}-independent transient outward K^+ current in rat ventricle. *J Physiol (Lond)* **500:**51–64.

Frech GC, VanDongen AM, Schuster G, Brown AM, and Joho RH (1989) A novel potassium channel with delayed rectifier properties isolated from rat brain by expression cloning. *Nature (Lond)* **340:**642–645.

Grissmer S, Nguyen AN, Aiyar J, Hanson DC, Mather RJ, Gutman GA, Karmilowicz MJ, Auperin DD, and Chandy KG (1994) Pharmacological characterization of five cloned voltage-gated K^+ channels, types Kv1.1, 1.2, 1.3, 1.5, and 3.1, stably expressed in mammalian cell lines. *Mol Pharmacol* **45:**1227–1234.

Hidalgo P and MacKinnon R (1995) Revealing the architecture of a K^+ channel pore through mutant cycles with a peptide inhibitor. *Science (Wash DC)* **268:**307–310.

Hulme JT, Coppock EA, Felipe A, Martens JR, and Tamkun MM (1999) Oxygen sensitivity of cloned voltage-gated K^+ channels expressed in the pulmonary vasculature. *Circ Res* **85:**489–497.

Hwang PM, Fotuhi M, Bredt DS, Cunningham AM, and Snyder SH (1993) Contrasting immunohistochemical localizations in rat brain of two novel K^+ channels of the Shab subfamily. *J Neurosci* **13:**1569–1576.

Hwang PM, Glatt CE, Bredt DS, Yellen G, and Snyder SH (1992) A novel K^+ channel with unique localizations in mammalian brain: molecular cloning and characterization. *Neuron* **8:**473–481.

Jan LY and Jan YN (1989) Voltage-sensitive ion channels. *Cell* **56:**13–25.

Jan LY and Jan YN (1997) Cloned potassium channels from eukaryotes and prokaryotes. *Annu Rev Neurosci* **20:**91–123.

Lampe RA, Defeo PA, Davison MD, Young J, Herman JL, Spreen RC, Horn MB, Mangano TJ, and Keith RA (1993) Isolation and pharmacological characterization of omega-grammotoxin SIA, a novel peptide inhibitor of neuronal voltage-sensitive calcium channel responses. *Mol Pharmacol* **44:**451–460.

Li-Smerin Y and Swartz KJ (1998) Gating modifier toxins reveal a conserved struc-

Downloaded from molpharm.aspetjournals.org by guest on December 1, 2012

tural motif in voltage- gated Ca^{2+} and K^+ channels. *Proc Natl Acad Sci USA* **95:**8585–8589.
Lim ST, Antonucci DE, Scannevin RH, and Trimmer JS (2000) A novel targeting signal for proximal clustering of the Kv2.1 K^+ channel in hippocampal neurons. *Neuron* **25:**385–397.
Marvin L, De E, Cosette P, Gagnon J, Molle G, and Lange C (1999) Isolation, amino acid sequence and functional assays of SGTx1. The first toxin purified from the venom of the spider *scodra griseipes*. *Eur J Biochem* **265:**572–579.
Miller C (1995) The charybdotoxin family of K^+ channel-blocking peptides. *Neuron* **15:**5–10.
Moczydlowski E, Lucchesi K, and Ravindran A (1988) An emerging pharmacology of peptide toxins targeted against potassium channels. *J Membr Biol* **105:**95–111.
Murakoshi H and Trimmer JS (1999) Identification of the Kv2.1 K^+ channel as a major component of the delayed rectifier K^+ current in rat hippocampal neurons. *J Neurosci* **19:**1728–1735.
Norton RS and Pallaghy PK (1998) The cystine knot structure of ion channel toxins and related polypeptides. *Toxicon* **36:**1573–1583.
Pak MD, Baker K, Covarrubias M, Butler A, Ratcliffe A, and Salkoff L (1991a) mShal, a subfamily of A-type K^+ channel cloned from mammalian brain. *Proc Natl Acad Sci USA* **88:**4386–4390.
Pak MD, Covarrubias M, Ratcliffe A, and Salkoff L (1991b) A mouse brain homolog of the *Drosophila* Shab K^+ channel with conserved delayed-rectifier properties. *J Neurosci* **11:**869–880.
Patel AJ, Lazdunski M, and Honore E (1997) Kv2.1/Kv9.3, a novel ATP-dependent delayed-rectifier K^+ channel in oxygen-sensitive pulmonary artery myocytes. *EMBO (Eur Mol Biol Organ) J* **16:**6615–6625.
Patel AJ, Lazdunski M, and Honore E (1999) Kv2.1/Kv9.3, an ATP-dependent delayed-rectifier K^+ channel in pulmonary artery myocytes. *Ann NY Acad Sci* **868:**438–441.
Pennington MW, Byrnes ME, Zaydenberg I, Khaytin I, de Chastonay J, Krafte DS, Hill R, Mahnir VM, Volberg WA, Gorczyca W, et al. (1995) *Chem* synthesis and characterization of ShK toxin: a potent potassium channel inhibitor from a sea anemone. *Int J Pept Protein Res* **46:**354–358.
Pongs O (1992) Molecular biology of voltage-dependent potassium channels. *Physiol Rev* **72:**S69–S88.
Rehm H, Bidard JN, Schweitz H, and Lazdunski M (1988) The receptor site for the bee venom mast cell degranulating peptide. Affinity labeling and evidence for a common molecular target for mast cell degranulating peptide and dendrotoxin I, a snake toxin active on K^+ channels. *Biochemistry* **27:**1827–1832.
Rehm H and Lazdunski M (1988) Purification and subunit structure of a putative K^+-channel protein identified by its binding properties for dendrotoxin I. *Proc Natl Acad Sci USA* **85:**4919–4923.
Salinas M, Duprat F, Heurteaux C, Hugnot JP, and Lazdunski M (1997) New modulatory alpha subunits for mammalian Shab K^+ channels. *J Biol Chem* **272:**24371–24379.
Sanguinetti MC, Johnson JH, Hammerland LG, Kelbaugh PR, Volkmann RA, Saccomano NA, and Mueller AL (1997) Heteropodatoxins: peptides isolated from spider venom that block Kv4.2 potassium channels. *Mol Pharmacol* **51:**491–498.
Schweitz H, Bruhn T, Guillemare E, Moinier D, Lancelin JM, Beress L, and Lazdunski M (1995) Kalicludines and kaliseptine. Two different classes of sea anemone toxins for voltage sensitive K^+ channels. *J Biol Chem* **270:**25121–25126.
Serodio P and Rudy B (1998) Differential expression of Kv4 K^+ channel subunits mediating subthreshold transient K^+ (A-type) currents in rat brain. *J Neurophysiol* **79:**1081–1091.
Swartz KJ and MacKinnon R (1995) An inhibitor of the Kv2.1 potassium channel isolated from the venom of a Chilean tarantula. *Neuron* **15:**941–949.
Swartz KJ and MacKinnon R (1997a) Hanatoxin modifies the gating of a voltage-dependent K^+ channel through multiple binding sites. *Neuron* **18:**665–673.
Swartz KJ and MacKinnon R (1997b) Mapping the receptor site for hanatoxin, a gating modifier of voltage-dependent K^+ channels. *Neuron* **18:**675–682.
Takahashi H, Kim JI, Min HJ, Sato K, Swartz KJ, and Shimada I (2000) Solution structure of hanatoxin1, a gating modifier of voltage-dependent K^+ channels: common surface features of gating modifier toxins. *J Mol Biol* **297:**771–780.
Tytgat J, Chandy KG, Garcia ML, Gutman GA, Martin-Eauclaire MF, van der Walt JJ, and Possani LD (1999) A unified nomenclature for short-chain peptides isolated from scorpion venoms: alpha-KTx molecular subfamilies. *Trends Pharmacol Sci* **20:**444–447.
Winterfield JR and Swartz KJ (2000) A hot spot for the interaction of gating modifier toxins with voltage- dependent ion channels. *J Gen Physiol* **116:**637–644.
Xu C, Lu Y, Tang G, and Wang R (1999a) Expression of voltage-dependent K^+ channel genes in mesenteric artery smooth muscle cells. *Am J Physiol* **277:**G1055–G1063.
Xu H, Barry DM, Li H, Brunet S, Guo W, and Nerbonne JM (1999b) Attenuation of the slow component of delayed rectification, action potential prolongation and triggered activity in mice expressing a dominant-negative Kv2 alpha subunit. *Circ Res* **85:**623–633.

Address correspondence to: Prof. Michel Lazdunski, Institut de Pharmacologie Moléculaire et Cellulaire, CNRS-UMR6097, 660 Route des Lucioles, Sophia-Antipolis, 06560 Valbonne, France. E-mail: ipmc@ipmc.cnrs.fr

MOL PHARM
MOLECULAR PHARMACOLOGY
aspet
Downloaded from molpharm.aspetjournals.org by guest on December 1, 2012